Comparison of antimony and arsenic behavior in an Ichinokawa River water-sediment system

Asaoka, Satoshi
Takahashi, Yoshio
Araki, Yusuke
Tanimizu, Masaharu

(Citation)
Chemical Geology,334:1-8

(Issue Date)
2012-12-12

(Resource Type)
journal article

(Version)
Accepted Manuscript

(URL)
https://hdl.handle.net/20.500.14094/90003332

Comparison of antimony and arsenic behavior in an Ichinokawa river water-sediment system

Satoshi Asaoka,[1,*,†] Yoshio Takahashi,[1] Yusuke Araki,[1] and Masaharu Tanimizu[2]

1) Department of Earth and Planetary Systems Science, Graduate School of Science, Hiroshima University, 1-3-1 Kagamiyama, Higashi-Hiroshima, Japan 739-8526

2) Kochi Institute for Core Sample Research, Japan Agency for Marine-Earth Science and Technology 200 Monobe Otsu, Nankoku, Japan 783-8502

[†]Present address: Research Center for Inland Seas, Kobe University 5-1-1 Fukaeminami, Higashinada, Kobe, Japan 658-0022

*CORRESPONDING AUTHOR

Tel: +81-78-431-6357

Fax: +81-78-431-6357

E-Mail: s-asaoka@maritime.kobe-u.ac.jp

Abstract

This study has demonstrated the similarities in the geochemical behavior of Sb and As under relatively oxic condition within a river system of Kamo-Ichinokawa in Japan. Speciation data in both water and solid phases were obtained by HPLC-ICP-MS and X-ray absorption fine structure analyses, respectively. The solid-water distributions of Sb and As are similar at all sampling points. Scavenging of the two elements from the aqueous phase was attributed to their adsorption onto iron (hydr)oxides. The two elements were finally incorporated into the river sediments where the host phases of Sb and As were determined by XAFS and sequential extraction experiments. The contribution of Sb and As adsorption onto particulate matters in the river water was relatively small, suggesting that the two elements are conservative under river water oxic conditions (Eh > 200 mV). The distribution coefficients of Sb and As for river water and river sediments were within a factor of 4.7 under oxic conditions. In our model calculations, however, their distribution coefficients largely differed by more than a factor of 25 to 50 under reducing conditions (Eh < 90 mV). This could be extended to infer the origin of As in natural systems under oxic conditions based on the As/Sb ratio where Sb and As behave similarly.

Keywords

antimony, arsenic, ferrihydrite, geochemical tracer, Ichinokawa Mine, XAFS

1. Introduction

Antimony (Sb) exists mainly as Sb(III) and Sb(V) in environmental, biological, and geochemical samples (Filella et al., 2002a). The average antimony concentrations in fresh water and seawater are 1.1 and 0.18 μg L^{-1}, respectively (Kharkar et al., 1968; Filella et al., 2002b), whereas those in sediments and soils are a few μg g^{-1} (Filella et al., 2002b). In industries, antimony is used as flame retardants, catalysts in plastics, pigments in paints, and additives in glassware, ceramics, ammunitions, and batteries (Herbst et al., 1985; Filella et al., 2002b). Plastic bottles contain a large amount of antimony with concentrations of 154-275 mg kg^{-1} (Takahashi et al., 2008). Hence, antimony is released into the environment through their disposal and combustion processes. It is reported that inhalation of antimony trisulfide or tyrioxide, as well as metallic Sb dust can cause lung tumors (Beyersmann and Hartwig, 2008). Therefore, it is very important to reveal the distribution and transport behavior of antimony in the environment.

Antimony and arsenic are considered to have similar geochemical properties such as distribution between river water and river sediment and transportation behavior in river water because the two elements belong to the same chemical group. Although numerous reports on arsenic contamination in groundwater have been recently published, the source of arsenic and its contamination mechanisms remain unclear (e.g., Polizzotto et al., 2003; Chauhan et al., 2009; Itai et al., 2010; Camacho et al., 2011). The number of studies on the distribution of arsenic and antimony in rivers, estuaries, ocean, soils and hydrothermal basin has increased over recent years (e.g., Byrd, 1990; Tighe et al., 2005; Manaka et al., 2007; Etter et al., 2007; Masson et al., 2009; Denys et al., 2009). Recently, Willis et al. (2011) discussed the two elements concentrations and speciation along flow paths in three groundwater flow systems in USA. However, previous studies have not addressed why geochemical behavior of the two redox sensitive elements is similar or has not considered their oxidation states.

The purpose of this study is to clarify the distribution and transport behavior of antimony between river water and the sediments based on oxidation states and adsorption characteristics using HPLC-ICP-MS and X-ray absorption fine structure (XAFS) and comparing these with arsenic.

2. Materials and Methods

2.1. Study site

The Ichinokawa Mine, abandoned in 1957, was one of the largest stibnite sources in the world, and its river systems are located in Saijo City (33.53°N, 133.12°E), Japan (Bancroft, 1988; Fig. 1). The mine can be regarded as a point source of antimony and arsenic as it is a low-temperature hydrothermal antimony deposit formed by Miocene hydrothermal activities. Sampling stations I-1 to I-3 in Ichinokawa river are affected by significant antimony loads from Ichinokawa mine and tributaries which flow through the antimony deposit. The Ichinokawa River is confluent with the Kamo River, which does not have any known antimony sources (St. K-1 and K-2) before its confluence with Ichinokawa River. After the confluence with Ichinokawa River, the downstream of Kamo River (St. K-3 to K-5) can be significantly affected by antimony loads from Ichinokawa river.

2.2. Sampling and analyses

River water samples were filtered through a 0.45 μm PTFE membrane filter (DISMIC, Advantec Ltd.) to separate dissolved and particulate matter fractions. Ultrapure analytical grade HNO_3 (TAMAPURE-AA-10, Tama Chemicals Co., Ltd.) was added to the filtrates to create 2 wt.% HNO_3 solution and stored in the dark at 4 °C until analysis. The concentrations of arsenic in the river samples were analyzed by a collision cell ICP-MS (7500, Agilent Technologies) to reduce interference of the $^{40}Ar^{35}Cl$ signal. Antimony in river samples was concentrated and purified using a modified thiol cotton fiber method before ICP-MS analysis (Asaoka et al., 2011).

The concentration of major ions was determined using an ion chromatograph (IC7000, Yokogawa Electric Corporation) employing Shodex IC YK-421 (Showa Denco K.K.) and Shim-pack IC-SA1/-SA1(G) (Shimadzu GLC Ltd.) columns for the cations and anions, respectively.

Antimony and arsenic speciation in water samples was determined using a HPLC-ICP-MS (HPLC pump, Pu-2089, JASCO) with a column oven (Co-2065 Plus, JASCO). An anion-exchange column (TSKgel super IC-AP, Tosoh) for antimony and arsenic speciation was used with 20 mM EDTA at pH

119 4.7 (Krachler and Emons, 2001). Standard solutions of Sb(III) , Sb(V), As(III) and As(V) were
120 prepared by dissolving appropriate amounts of potassium antimony tartrate, $KSb(OH)_6$, $KAsO_2$ and
121 KH_2AsO_4, respectively, in ultra pure water.
122 River sediments were collected as follows: the river sediments and river water were successively
123 sifted together through a screen (1 mm) to remove gravel and a sieve (180 μm), dried in an oven at
124 40 °C for 3 days, after which the sediments (0.18 mm~< 1 mm) and particulate matters (>0.45 μm) from
125 the river water were digested with HF-$HClO_4$-HNO_3 solutions (Takahashi et al., 2002). Thereafter, the
126 sample was evaporated at 160 °C and subsequent digestion was conducted with $HClO_4$ solution and 6
127 mol L^{-1} HCl solution. The evaporation process between each digestion was consistently conducted at
128 160 °C to prevent Sb and As loss. The digested solution was prepared as 2% HNO_3 solution for ICP-
129 MS analysis (7500, Agilent Technologies). The river sediment samples for XAFS analysis were sealed
130 immediately in polystyrene bottles and transported to the laboratory in the dark at 4 °C. In the
131 laboratory, the river sediment samples were packed into polyethylene bags under N_2 gas atmosphere
132 and stored at -20 °C to maintain oxidation state before XAFS analysis. Antimony and arsenic K-edge
133 XAFS spectra (energy range 30.15-30.85 keV, adsorption edge 30.487 keV for Sb; energy range 11.78-
134 12.20 keV, adsorption edge 11.865 keV for As) were measured by X-ray fluorescence yield mode using
135 a 19-element Ge semiconductor detector at BL01B1 with Si(311) and Si(111) double-crystal
136 monochromator and two mirrors at SPring-8, Japan. Sb_2O_3, $KSb(OH)_6$, $NaAsO_2$, and NaH_2AsO_4 (Wako
137 Pure Chemicals) were measured by transmission mode as standards for Sb(III), Sb(V), As(III), and
138 As(V), respectively. Least-squares fitting of X-ray absorption near edge structure (XANES) spectra
139 with linear combination of reference spectra was performed with a REX2000 software (Rigaku Co.) to
140 estimate Sb(III)/Sb(V) and As(III)/As(V) ratios in solid samples (Mitsunobu et al., 2006; Takahashi et
141 al., 2008). The iron XAFS spectra were measured to identify iron minerals in the river sediments,
142 which were measured by fluorescence yield mode using a Lytle detector at BL12C in Photon Factory,
143 KEK, Japan by using a Si(111) double crystal monochromator and a bent cylindrical mirror. Extended
144 X-ray absorption fine structure (EXAFS) data were analyzed using a REX2000 (Rigaku Co.). The

145 theoretical phase shift and amplitude functions employed in this fitting procedure were extracted by
146 FEFF 7.0 (Zabinsky et al., 1995). The error estimates of the fitted parameters in bond distance and
147 coordination number were ±0.02 Å and ±20%, respectively (Mitsunobu et al., 2006). To identify the
148 host phase, sequential extraction was also conducted following Tessier et al. (1979).
149
150 **3. Results and Discussion**
151 **3. 1. Antimony and arsenic in river water.**
152 The concentration of major ions such as Cl^- , NO_3^-, SO_4^{2-}, Na^+, Ca^{2+} and Mg^{2+} ranged between 2.7 to
153 3.7, 3.0 to 4.3, 7.6 to 17.9, 4.1 to 6.8, 11.8 to 15.3 and 1.5 to 4.7 mg L^{-1}, respectively (Table 1). The
154 concentrations of major ions did not quite differ among sampling stations. Sulfate concentrations in the
155 Ichinokawa River (St. I-1~3) were larger than those in the Kamo River, possibly due to the supply of
156 sulfate by the oxidation of abundant sulfide in the Ichinokawa Mine.
157 The concentrations of antimony in the upstream portions of the Kamo River where identifiable
158 sources of antimony are lacking (i.e., St. K-1 and K-2) range from 0.16 to 0.19 μg L^{-1} (Fig. 2A),
159 whereas those in Ichinokawa River (St. I-1~3) were 13.6-113 μg L^{-1}, which were 2 to 3 orders of
160 magnitude higher than those in Kamo River. In particular, at St. I-2, the concentration increased
161 dramatically after flowing down to Ichinokawa Mine, indicating that a significant amount of antimony
162 is discharged from the mine. The concentration of SO_4^{2-} was correlated (r=0.987) with that of the
163 antimony in this river system, suggesting the dissolution (oxidation) of stibnite as a source of antimony
164 from the abandoned mine. Antimony concentrations in the downstream of Kamo River after confluence
165 with Ichinokawa River (St. K-4 and K-5) were 3.90 and 4.30 μg L^{-1}, respectively, which increased by
166 more than 1 order of magnitude compared with the river water in the Kamo River before the confluence.
167 The oxidation state of antimony in all the river samples determined by the HPLC-ICP-MS analyses was
168 pentavalent possibly, dissolved as $Sb(OH)_6^-$ (Fig. S1).
169 Similar results were observed for arsenic. The concentrations of arsenic in the upstream of the Kamo
170 River (St. K-1 and K-2) were 0.29 and 0.28 μg L^{-1}, respectively (Fig. 2B), whereas the concentrations in

Ichinokawa River for St. I-1, 2, and 3 were 0.86, 3.9 and 3.2 μg L^{-1}, respectively. The HPLC-ICP-MS analyses showed that the major arsenic oxidation state in river water was pentavalent, corresponding to $H_2AsO_4^-$ (Fig. 3). Both antimony and arsenic are mainly pentavalent because the pentavalent species is thermodynamically stable under this river system condition (pH: 6.6 to 7.0; Eh: 390-414 mV; Vink, 1996).

The variations in concentrations of antimony and arsenic are similar (Figs. 2A, 2B), given that the correlation coefficients (r) for both concentrations were 0.974 (Fig. 4A). The mass balance of antimony, arsenic, and major elements was calculated by their loads at St. K-2, I-3 and K-4 (Table 2). The loads of the major elements were conserved before (St. K-2 and I-3) and after (St. K-4) the confluence of the two rivers, considering that the percentage of the excess or deficiency between the sums of K-2 and I-3 loads and K-4 (after the confluence of the two rivers) was within -5.1–14%. In contrast, the antimony and arsenic loads at St. K-4 after the confluence of the two rivers were 29% and 20% smaller than those before confluence (=K-2 + I-3), indicating that the two elements were scavenged to some degree from the river water due to adsorption onto river sediments or suspended solids until reaching St. K-4.

The distribution coefficients (K_d) between the particulate matter and dissolved fractions at St. K-2, I-3, and K-4 were calculated (Table 3). K_d (L kg^{-1}) is defined as C_p/C_d, where C_p is the concentration of antimony or arsenic in the particulate matter fraction (μg kg^{-1}) and C_d is the concentration in the dissolved fraction (μg L^{-1}). The K_d for antimony was lower than that for arsenic, showing that arsenic has a higher affinity with the particulate matter compared with antimony in the river system where the two elements have been mainly dissolved as pentavalent species. Nevertheless, more than 97-99% of arsenic and antimony were distributed to the dissolved fraction in the aqueous phase because the particulate antimony and arsenic concentrations in river water were 0.00007-0.004 μg L^{-1} and 0.002-0.009 μg L^{-1}, respectively. Therefore, the contributions of adsorption onto suspended solids in the river systems were relatively small.

3.2. Antimony and arsenic in river sediment.

196 The concentration of antimony in the upstream sediments of Kamo River (St. K-1 and K-2) was
197 around 0.1-0.2 mg kg^{-1}, whereas that in Ichinokawa River (St. I-1~3) was 71.6-531 mg kg^{-1} (i.e., 3 to 4
198 orders of magnitude higher; Fig. 2C). Arsenic concentration showed a similar trend with antimony at
199 18.1-88.3 mg kg^{-1} for St. I-1~3; this was 1 to 2 orders of magnitude higher than in the upstream part of
200 Kamo River (Fig. 2D). Antimony concentration in the downstream sediments of Kamo River after the
201 confluence with Ichinokawa River (St. K-4 and K-5) increased by more than 1 order of magnitude
202 compared with the sediments in the Kamo River before confluence. Similar results were also observed
203 for arsenic; the correlation coefficient between antimony and arsenic was 0.992 (Fig. 4B).
204 Sb(III)/Sb(V) ratio calculated by the XANES spectra showed that 60 to 84% of antimony in the
205 sediments are pentavalent (Fig. 5A, Table S1). The arsenic XANES spectra of the river sediments were
206 measured only for the samples from St. I-1 to 3 due to their lower As concentrations, showing that 78%
207 of arsenic in the river sediments was pentavalent (Fig. 5B, Table S2). These results showed that
208 pentavalent antimony and arsenic are dominant species in the river sediments.
209 Antimony and arsenic concentrations in the sediments also correlated well with those in the river
210 water (Figs. 6; r=0.970 and 0.991 for arsenic and antimony, respectively). Under reducing condition,
211 Sb and As can be precipitated as arsenopyrite and stibnite, respectively (Wilson et al., 2004), but this is
212 unlikely because these sulfides are not stable under the oxic condition of this river system (pH: 6.6 to
213 7.0; Eh: 390-414 mV) . These results suggest that antimony or arsenic concentration in aqueous phase
214 was controlled by adsorption. Notably, the adsorption reaction is very important for the solid-water
215 distributions of these elements in the system. The distribution coefficients (K_d) of antimony and arsenic
216 between river water and river sediments were apparent at 8.8×10^2 -9.0×10^3 L kg^{-1} and 2.0×10^3- $2.2 \times$
217 10^4 L kg^{-1}, respectively (Fig. S2). The K_d values for antimony and arsenic between river water and river
218 sediments were similar to those between water and particulate matter (Table 3; Fig. S2).
219 The host phases of antimony and arsenic in the river sediments can be iron hydroxides (e.g., Landrum
220 et al., 2009; Mitsunobu et al., 2010). To quantify iron mineral in the river sediments, several XAFS
221 spectra of iron minerals at Fe K-edge such as ferrihydrite, biotite, hematite, and magnetite were

compared to those of the river sediments. The combination fit using ferrihydrite and biotite concurred well with the iron XANES of the river sediments. Iron K-edge XANES of the river sediments showed that 42-67% of the iron in the river sediments was ferrihydrite (Fig. 7; Table S3). Because it is reported that the point of zero charge of ferrihydrite is about pH 8 (Trivedi, 2003; Hiemstra and Riemsdijk, 2009), the ferrihydrite in river sediments could be positively charged at pH 6.9 in the river water. The $Sb(OH)_6^-$, a possible major species of dissolved antimony, could be adsorbed onto ferrihydrite in the river sediments. Arsenic was also charged negatively (e.g., $H_2AsO_4^-$), and this could be adsorbed onto ferrihydrite. To confirm the host phases, the Sb EXAFS spectrum for the sediments at St. I-2, which exhibits the highest concentration of antimony, was measured. According to the parameter fitting of the k^3-weighted EXAFS spectrum (Fig. 8; Table 4), the spectra can be fitted by Sb-O, Sb-Fe1 (second shell), and Sb-Fe2 (third shell) shells, which shows that their distances were 1.99, 3.12, and 3.61 Å, respectively. The results agreed well with those reported for Sb adsorbed on ferrihydrite (Mitsunobu at al., 2010). This result agrees well with previous reports that ferrihydrite, or low crystalline iron (hydr)oxide, is a major host phase of antimony in river sediments (Craw et al, 2004).

Because arsenic EXAFS could not be obtained due to the low concentration, a sequential extraction experiment was conducted using the St. I-2 sediment (Table 5). Results showed that 60% and 18% of As were extracted in poorly crystalline iron (hydr)oxide or ferrihydrite fraction and more crystalline iron (hydr)oxide fraction, respectively. Therefore, the Fe (hydr)oxides are the major host phases of antimony and arsenic in the river sediments. These results can be also supported by previous EXAFS data of the sediments, showing the host phases of As in soil as Fe(III) hydroxide (Mitsunobu et al., 2006).

3.3. Comparison of solid-water distributions between antimony and arsenic

Results from this study showed that variations in concentrations of antimony and arsenic in river water and sediments were well correlated each other. The EXAFS and sequential extraction results showed that iron (hydr)oxides acted as host phases of these elements. All results implied that the

248 distribution and migration of antimony and arsenic in the river-sediment system were similar, at the
249 minimum, under oxic conditions. In this study, the oxidation state of antimony and arsenic in the river
250 water and river sediments was confirmed using HPLC-ICP-MS and XAFS, respectively, which allowed
251 us to calculate concentrations of Sb(III), Sb(V), As(III) and As(V) and accordingly estimate the K_d
252 values independently for trivalent or pentavalent states. The apparent K_d values for Sb(V), As(V), and
253 As(III) were obtained based on the results of St. I-2; $K_{d\text{-}Sb(V)}=4.3\times10^3$ (L kg^{-1}), $K_{d\text{-}As(V)}=2.0\times10^4$ (L kg^{-1}),
254 and $K_{d\text{-}As(III)}=4.5\times10^4$ (L kg^{-1}). Sb(III) was not detected in the HPLC-ICP-MS analysis of the river
255 water; consequently, we could not obtain the $K_{d\text{-}Sb(III)}$ value. However, the possible minimum value was
256 calculated as $K_{d\text{-}Sb(III)} > 1.1\times10^6$ (L kg^{-1}), taking into account the detection limit of Sb(III) in the HPLC-
257 ICP-MS measurement. With the results, the apparent K_d values of antimony and arsenic at various
258 redox conditions were calculated at pH 7 (Fig. 9). The oxidation states of antimony and arsenic as a
259 function of Eh were calculated by Visual MINTEQ ver. 2.61 (Gustafsson, 2010). Under oxic conditions,
260 where Sb(V) and As(V) are the main species (Eh > 200 mV; pH 7), the apparent K_d values were similar
261 within the factor of 4.7. At Eh from 0 to 90 mV (pH 7), the major species were found as Sb(III) and
262 As(V); the difference in apparent K_d values between antimony and arsenic was by more than a factor of
263 50. This indicated that both antimony and arsenic were fractionated under reducing conditions by a
264 larger degree than under oxic conditions. At Eh less than -10 mV (pH 7), the major species were found
265 as Sb(III) and As(III); the apparent K_d value of arsenic was less than that of antimony by more than a
266 factor of 25. The factor could even be larger, as the $K_{d\text{-}Sb(III)}$ employed by the present study was a
267 minimum value. The results supported the earlier finding that solid-water distribution of antimony is
268 relatively similar to that of arsenic under oxic conditions, such as in the river-sediment system presented
269 by this study (Eh; 390-414 mV), but not under reducing conditions. A similar Sb and As chemical
270 behavior in water is reported in the Nishinomaki Mine, Japan under oxic conditions (pH=3.26–7.05,
271 Eh=550–750 mV; Manaka et al., 2007), as presented in Fig. 9. They reported that antimony was
272 attenuated by iron-bearing ocherous precipitates, especially schwertmannite. The variations in
273 concentrations of antimony and arsenic in the drainage water were quite similar along the stream.

Variations in concentrations of antimony and arsenic in water up to the Sb smelting site were also similar in an Sb mining area in Hunan, China (Fu et al., 2010). Furthermore, similar variations and seasonal changes in the distribution of the two elements were observed in the Garonne and Dordogne branches which are part of the largest fluvial estuarine system in Europe (ave. pH=7.8-7.9, ave. Eh=184-316 mV; Masson et al, 2009) and in Waikato River, the longest river in New Zealand (pH=6.59-7.57, oxic condition; Wilson and Webster-Brown, 2009). Although the concentrations of the two elements in these river systems were also controlled by suspended matters, K_d values of the two elements to SPM were correlated (Masson et al, 2009; Wilson and Webster-Brown, 2009). Therefore, variations in the concentration of the two elements in those river systems are similar. These results confirmed that the two elements are similarly distributed between solid and water phases under oxic conditions.

In contrast, antimony was much less soluble than arsenic under reducing conditions (pH=6.6-6.8, Eh=40–120 mV; Mitsunobu et al., 2006). In suboxic or anoxic sediments in estuaries, the behavior of arsenic and antimony could be different. For example, the remobilization of arsenic and antimony might differ in suboxic or anoxic sediments (Byrd, 1990). These results are plausible as presented in Fig. 9, which shows that the apparent K_d value of arsenic was lower than that of antimony under reducing conditions.

Given that the redox conditions of river systems are generally oxic, the main species of antimony and arsenic in the river water and particulate matters (and sediments) are pentavalent. The distribution coefficients of antimony and arsenic between the river water and river sediments were similar within the factor of 4.7 under oxic conditions (Eh > 200 mV, accordingly. The scavenging of the two elements was also similar due to adsorption on iron (hydr)oxide. Consequently, the geochemical behavior of antimony and arsenic will be similar under oxic conditions (Eh > 200 mV). In other words, these results could be extended to identify specific As source in natural waters based on the As/Sb ratio where Sb and As behave similarly.

4. Conclusion

This study has demonstrated the similarities of the geochemical behavior of antimony and arsenic in the river system of Kamo-Ichinokawa, Japan. Results suggest that the scavenging of the two elements from the aqueous phase can be attributed to their adsorption onto iron (hydr)oxides. The calculated apparent K_d values of antimony and arsenic at various redox conditions considering their oxidation states suggests that under oxic conditions, where Sb(V) and As(V) are the main species, the apparent K_d values between river water and river sediments are similar within a factor of 4.7. Consequently, the geochemical behavior of antimony and arsenic will be similar under oxic conditions in river systems.

Acknowledgments

This research was supported by the Global Environment Research Fund of the Ministry of the Environment Japan (RF-084a) and by the Research Project for Ensuring Food Safety from Farm to Table AC-1110. XAFS measurements were performed with the approval of JASRI/SPring-8 (Proposal Nos. 2011B1742 and 2012A1299) and Photon Factory (2008G683 and 2009G655).

References

Asaoka, S., Takahashi, Y., Araki, Y., Tanimizu, M., 2011. Preconcentration method of antimony using modified thiol cotton fiber for isotopic analyses of antimony in natural samples, Analytical Sciences 27, 25-28

Bancroft, P., 1988. Famous mineral localities: the Ichinokawa mine, Mineralogical Record 19, 229-238.

Beyersmann, D., Hartwig, A., 2008. Carcinogenic metal compounds: recent insight into molecular and cellular mechanisms. Archives of Toxicology 82, 493-512

Byrd, J.T., 1990. Comparative geochemistries of arsenic and antimony in rivers and estuaries. Science of the Total Environment 97/98, 301-314.

325 Camacho, L.M., Gutiérrez, M., Alarcón-Herrera, M.T., de Lourdes Villalba, M., Deng, S., 2011.
326 Occurrence and treatment of arsenic in groundwater and soil in northern Mexico and southwestern
327 USA. Chemosphere 83, 211-225.

328 Chauhan, V.S., Nickson, R.T., Chauhan, D., Iyengar, L., Sankararamakrishnan, N., 2009. Ground water
329 geochemistry of Ballia district, Uttar Pradesh, India and mechanism of arsenic release. Chemosphere
330 75, 83-91.

331 Craw, D., Wilson, N., Ashley, P.M., 2004. Geochemical controls on the environmental mobility of Sb
332 and As at mesothermal antimony and gold deposits. Applied Earth Science 113, 3-10.

333 Denys, S., Tack, K., Caboche, J., Delalain, P., 2009. Bioaccessibility, solid phase distribution, and
334 speciation of Sb in soils and in digestive fluids. Chemosphere 74, 711-716.

335 Ettler, V., Mihaljevic, M., š ebek, O., Nechutný, Z., 2007. Antimony availability in highly polluted

336 soils and sediments - A comparison of single extractions. Chemosphere 68, 455-463.

337 Filella, M., Belzile, N., Chen, Y.W., 2002a. Antimony in the environment: a review focused on natural
338 waters: II. Relevant solution chemistry. Earth Science Reviews 59, 265-285.

339 Filella, M., Belzile, N., Chen, Y.W., 2002b. Antimony in the environment: A review focused on natural
340 waters I. Occurrence. Earth Science Reviews 57, 125-176.

341 Fu, Z., Wu, F., Amarasiriwardena, D., Mo, C., Liu, B., Zhu, J., Deng, Q., Liao, H., 2010. Antimony,
342 arsenic and mercury in the aquatic environment and fish in a large antimony mining area in Hunan,
343 China. Science of the Total Environment 408, 3403-3410.

344 Gustafsson, J.P. Visual MINTEQ, http://www.lwr.kth.se/english/OurSoftware/vminteq/index.htm,
345 Stockholm,Sweden, accessed September 2012

346 Herbst, K.A., Rose, G., Hanusch, K., Schumann, H., Wolf H.U., 1985. Antimony and antimony
347 compounds, In: Gerhartz, W.; Yamamoto, S.; Campbell, F.T.; Arpe, H.-J. (Eds.). Ullmann's
348 Encyclopedia of Industrial Chemistry vol. A3, fifth ed., Wiley-VCH, Weinheim, pp. 55-76.

349 Hiemstra, T., Riemsdijk, W.H.V., 2009. A surface structural model for ferrihydrite I: Sites related to
350 primary charge, molar mass, and mass density. Geochimica Cosmochimica Acta 73, 4423-4436.

351 Itai, T., Takahashi, Y., Seddique, A.A., Maruoka, T., Mitamura, M., 2010. Variations in the redox state
352 of As and Fe measured by X-ray absorption spectroscopy in aquifers of Bangladesh and their effect
353 on As adsorption. Applied Geochemistry 25, 34-47.

354 Kharkar, D.P., Turekian, K.K., Bertine K.K., 1968. Stream supply of dissolved silver, molybdenum,
355 antimony, selenium, chromium, cobalt, rubidium and cesium to the oceans. Geochimica
356 Cosmochimica Acta 32, 285-298.

357 Krachler, M., Emons, H., 2001. Urinary antimony speciation by HPLC-ICP-MS. Journal of Analytical
358 Atomic Spectrometry 16, 20-25.

359 Landrum, J.T., Bennett, P.C., Engel, A.S., Alsina, M.A., Pastén, P.A, Milliken, K., 2009. Partitioning
360 geochemistry of arsenic and antimony, El Tatio Geyser Field, Chile. Applied Geochemistry 24, 664-
361 676.

362 Manaka, M., Yanase, N., Sato, T., Fukushi, K., 2007. Natural attenuation of antimony in mine
363 drainage water. Geochemical Journal 41, 17-27.

364 Masson, M., Schäfer, J., Blanc, G., Dabrin, A., Castelle, S., Lavaux, G., 2009. Behavior of arsenic and
365 antimony in the surface freshwater reaches of a highly turbid estuary, the Gironde Estuary, France.
366 Applied Geochemistry 24, 1747-1756.

367 Mitsunobu, S., Harada, T., Takahashi, Y., 2006. Comparison of antimony behavior with that of arsenic
368 under various soil redox conditions. Environmental Science and Technology 40, 7270-7276.

369 Mitsunobu, S., Takahashi, Y., Terada, Y., Sakata M., 2010. Antimony(V) incorporation into synthetic
370 ferrihydrite, goethite, and natural iron oxyhydroxides. Environmental Science and Technology 44,
371 3712-3718.

372 Polizzotto, M. L., Kocar, B.D., Benner, S.G., Sampson, M., Fendorf, S., 2008. Near-surface wetland
373 sediments as a source of arsenic release to ground water in Asia. Nature 454, 505-508.

374 Takahashi, Y., Yoshida, H., Sato, N., Hama, K., Yusa, Y., Shimizu, H., 2002. W- and M- type tetrad
375 effects in REE patterns for water-rock systems in the Tono uranium deposit, central Japan, Chemical
376 Geology, 184, 311-335.

377 Takahashi, Y., Sakuma, K., Itai, T., Zheng, G., Mitsunobu, S., 2008. Speciation of antimony in PET
378 bottles produced in Japan and China by X-ray absorption fine structure spectroscopy. Environmental
379 Science and Technology 42, 9045-9050.

380 Tessier, A., Campbell, P.G.C., Bisson, M., 1979. Sequential extraction procedure for the speciation of
381 particulate trace metals. Analytical Chemistry 51, 844-851.

382 Tighe, M., Ashley, P., Lockwood, P., Wilson, S., 2005. Soil, water, and pasture enrichment of antimony
383 and arsenic within a coastal floodplain system. Science of the Total Environment 347, 175-186.

384 Trivedi, P., Dyer, J. A., Sparks, D.L., 2003. Lead sorption onto ferrihydrite. 1. A macroscopic and
385 spectroscopic assessment. Environmental Science and Technology 37, 908-914.

386 Vink, B.W., 1996. Stability relations of antimony and arsenic compound in the light of reversed and
387 extended Eh-pH diagrams. Chemical Geology 130, 21-30.

388 Willis, S.S, Haque, S.E., Johannesson, K.H., 2011. Arsenic and antimony in groundwater flow systems:
389 A comparative study. Aquatic Geochemistry 17, 775-807.

390 Wilson, N.J., Craw, D., Hunter, K., 2004. Antimony distribution and environmental mobility at an
391 historic antimony smelter site, New Zealand, Environmental Pollution 129, 257-266.

392 Wilson, N., Webster-Brown, J., 2009. The fate of antimony in a major lowland river system, the
393 Waikato River, New Zealand. Applied Geochemistry 24, 2283-2292.

394 Zabinsky, S.I., Rehr, J.J., Ankudinov, A., Albers, R.C., Eller M.J., 1995. Multiple-scattering
395 calculations of X-ray-absorption spectra. Physical Review B52, 2995-3009.

Figure Captions

Fig. 1 Map of study site and sampling stations in Kamo and Ichinokawa Rivers.

The Ichinokawa River is confluent with the Kamo River, which does not have any known antimony sources before its confluence with Ichinokawa River

Fig. 2 Concentrations of antimony (A) and arsenic (B) in Kamo and Ichinokawa Rivers, and those of antimony (C) and arsenic (D) in the sediments

Symbols: □ : Kamo River; ● : Ichinokawa River

Fig. 3 Arsenic species in Kamo and Ichinokawa Rivers.

Fig. 4 Correlation between concentrations of arsenic and antimony in Kamo and Ichinokawa river water (A) and in river sediments(B)

Fig. 5 Antimony (A) and arsenic (B) K edge XANES spectra of the river sediments of Kamo and Ichinokawa Rivers.

Sb_2O_3 and $Sb(OH)_6^-$ represent Sb(III) and Sb(V) standards, respectively.

$NaAsO_2$ and NaH_2AsO_4 represent As(III) and As(V) standards, respectively.

Fig. 6 Correlation between concentrations of antimony (A) and arsenic (B) in sediment and river water along Kamo and Ichinokawa river water.

Fig. 7 Iron K edge XANES spectra of Kamo and Ichinokawa river sediments

Fig. 8 Fourier transformed k^3-weighted EXAFS spectra of antimony in the river sediments of Ichinokawa River (St. I-2) in *k* space (A) and *R* space (B).

Fig. 9 Antimony and arsenic distribution coefficients between river water and river sediments under redox conditions.

Figures.

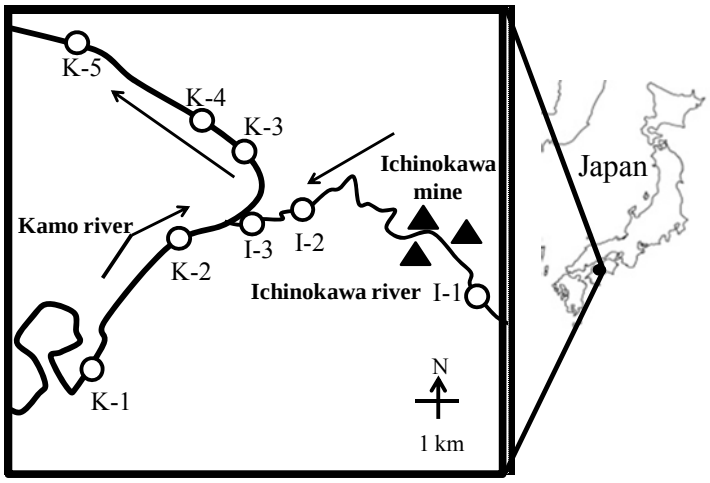

Fig. 1

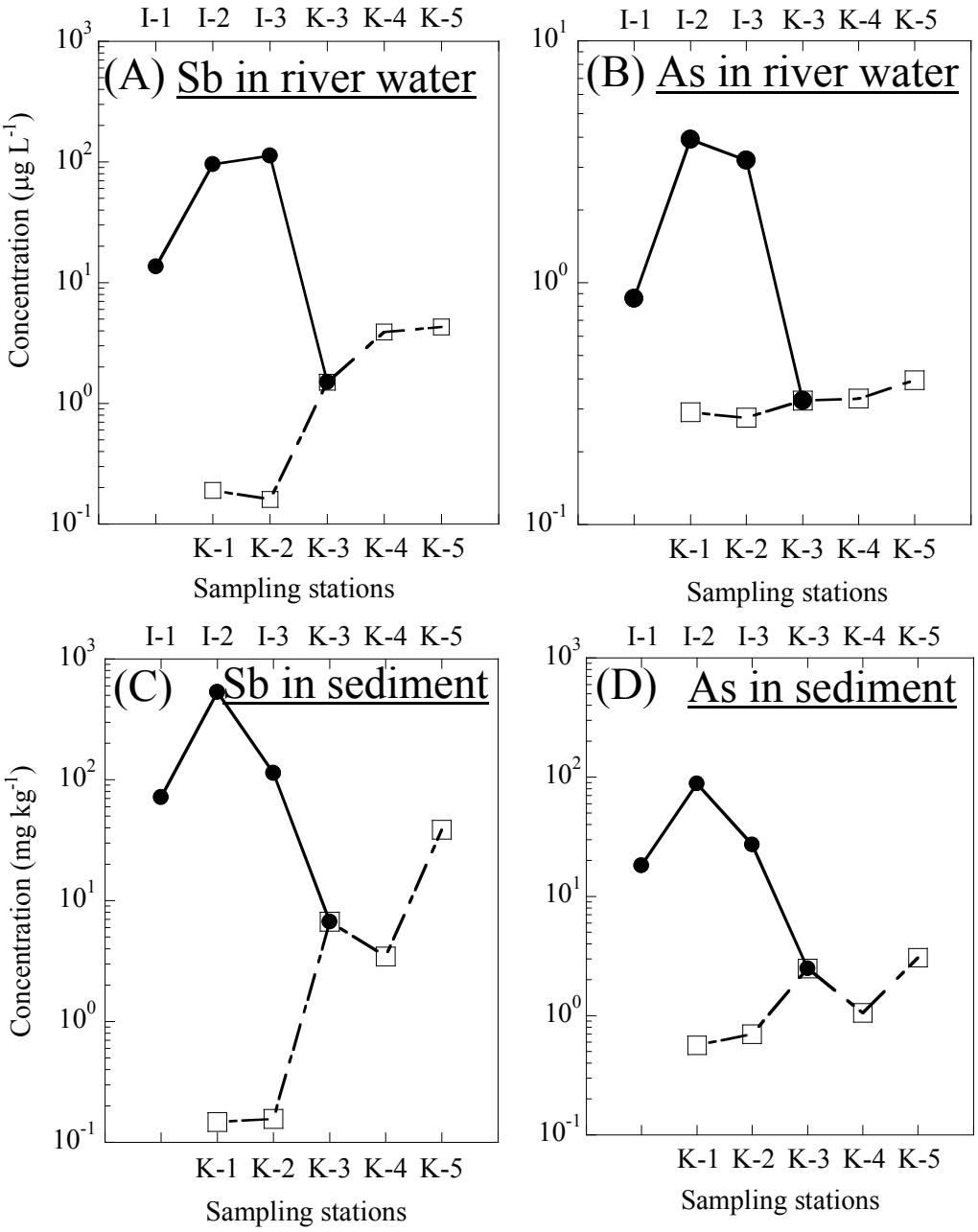
(A) Sb in river water
(B) As in river water
(C) Sb in sediment
(D) As in sediment
I-1 I-2 I-3 K-3 K-4 K-5
K-1 K-2 K-3 K-4 K-5
Sampling stations
Concentration (μg L-1)
Concentration (mg kg-1)

Fig. 2

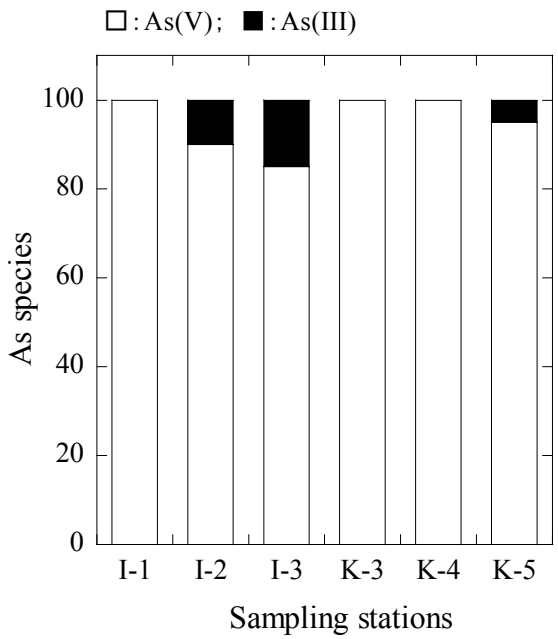
□ : As(V) ; ■ : As(III)
100
80
60
40
20
0
As species
I-1
I-2
I-3
K-3
K-4
K-5
Sampling stations

Fig. 3

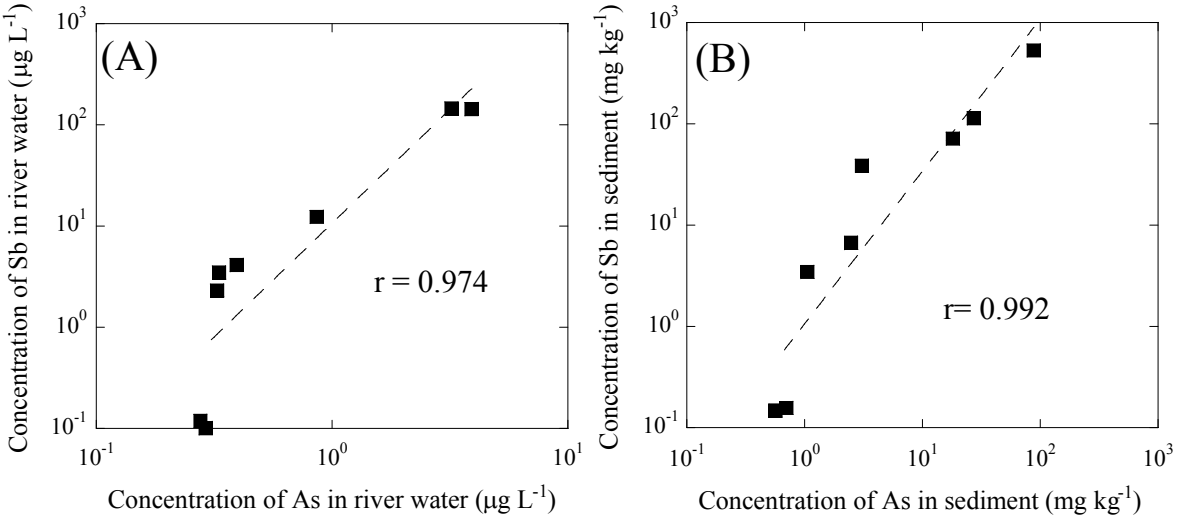
(A)
r = 0.974
Concentration of Sb in river water (μg L-1)
Concentration of As in river water (μg L-1)
(B)
r= 0.992
Concentration of Sb in sediment (mg kg-1)
Concentration of As in sediment (mg kg-1)

Fig. 4

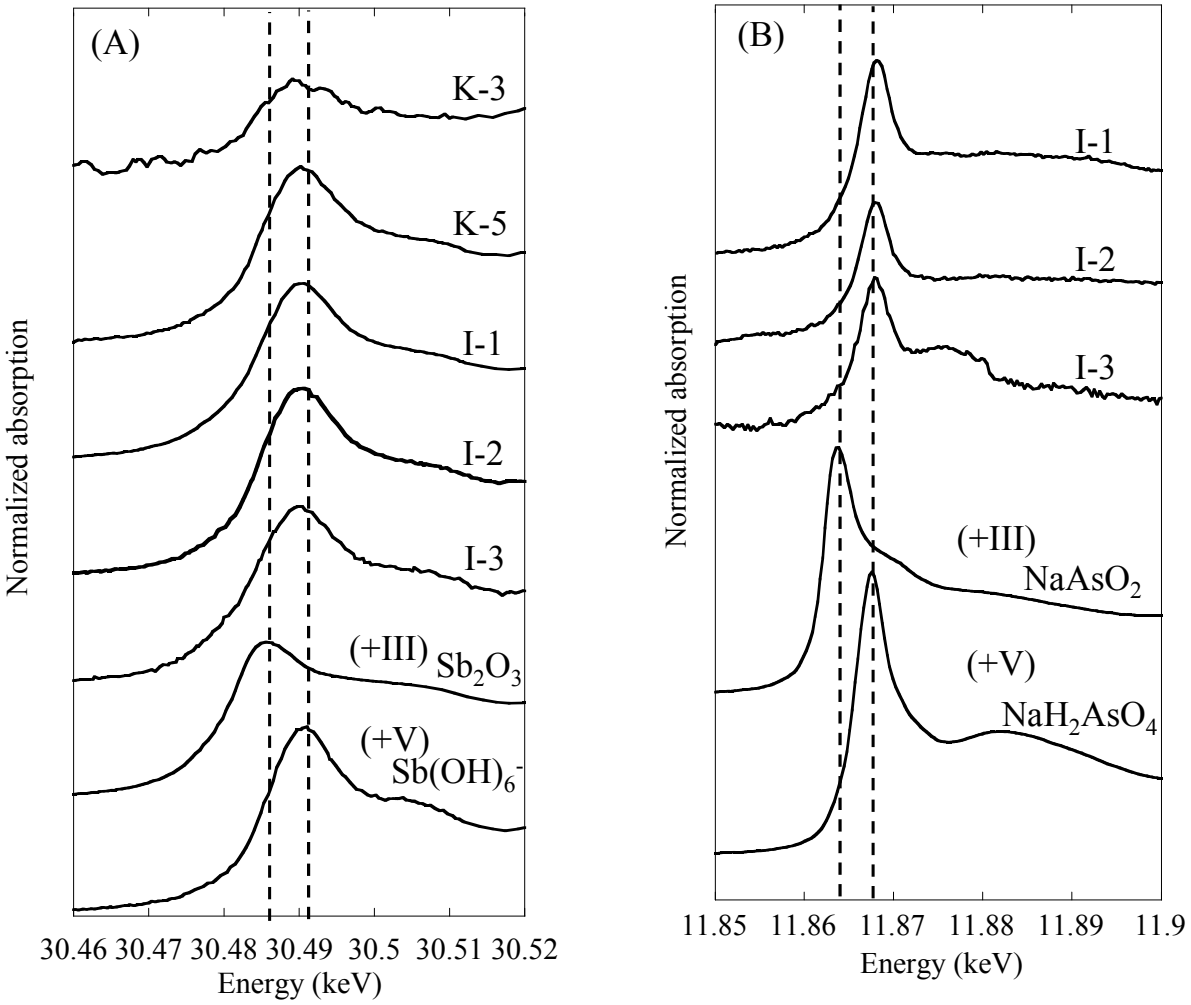
(A)
K-3
K-5
I-1
I-2
I-3
(+III) Sb_2O_3
(+V) $Sb(OH)_6^-$
Normalized absorption
30.46 30.47 30.48 30.49 30.5 30.51 30.52
Energy (keV)
(B)
I-1
I-2
I-3
(+III) $NaAsO_2$
(+V) NaH_2AsO_4
Normalized absorption
11.85 11.86 11.87 11.88 11.89 11.9
Energy (keV)

Fig. 5

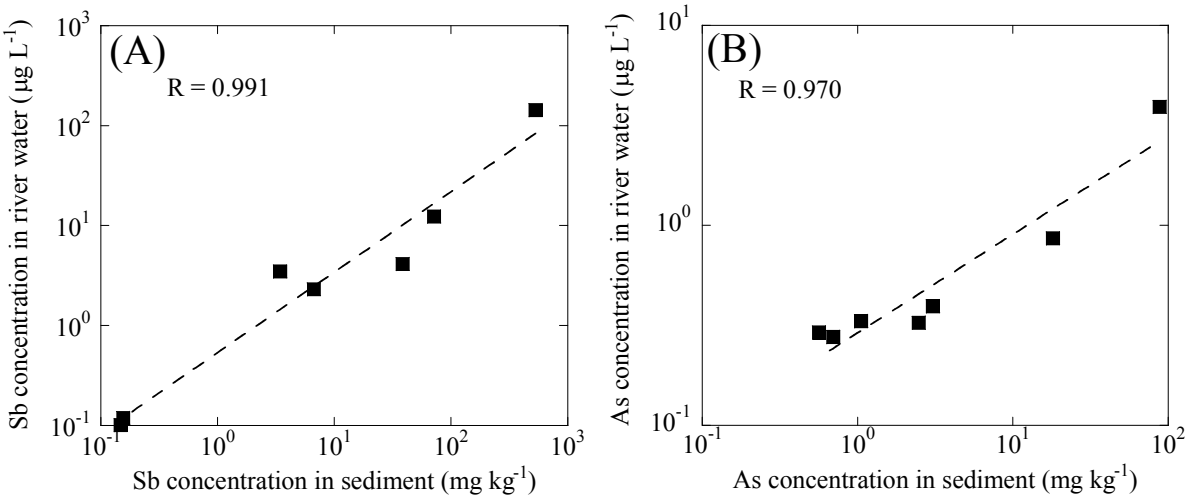
(A)
R = 0.991
Sb concentration in river water (μg L-1)
Sb concentration in sediment (mg kg-1)
(B)
R = 0.970
As concentration in river water (μg L-1)
As concentration in sediment (mg kg-1)

Fig. 6

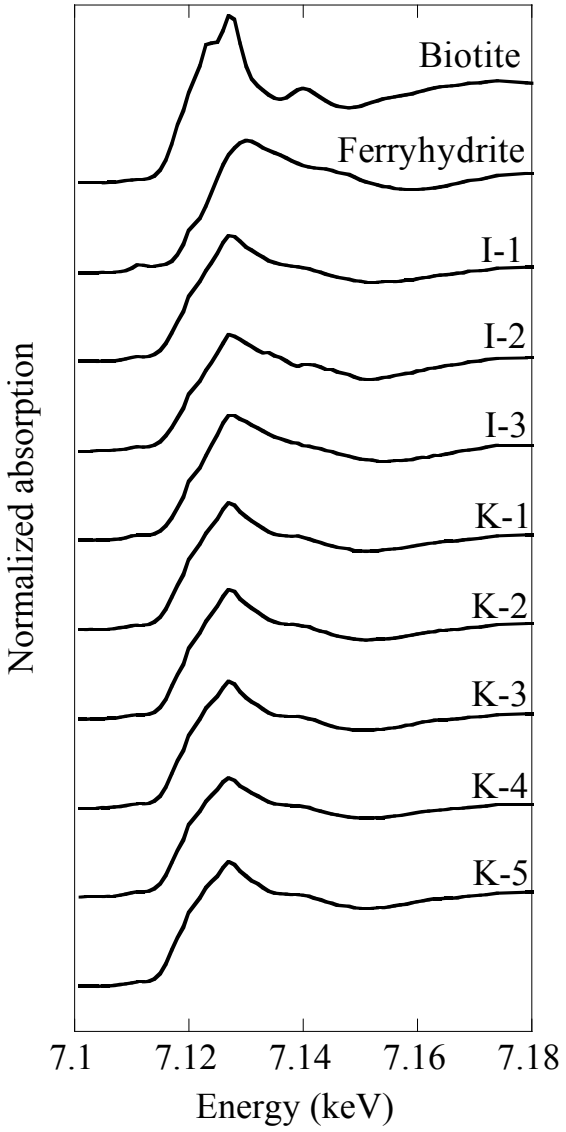
Biotite
Ferryhydrite
I-1
I-2
I-3
K-1
K-2
K-3
K-4
K-5
Normalized absorption
7.1
7.12
7.14
7.16
7.18
Energy (keV)

Fig. 7

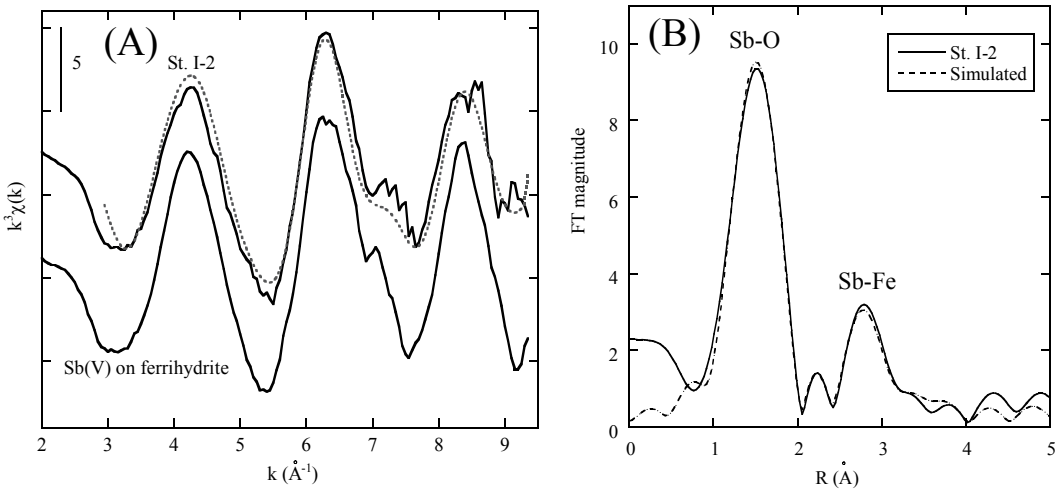
(A)
5
St. I-2
Sb(V) on ferrihydrite
k^{3}χ(k)
k (Å^{-1})
2
3
4
5
6
7
8
9
(B)
Sb-O
Sb-Fe
St. I-2
Simulated
FT magnitude
R (Å)
0
1
2
3
4
5
0
2
4
6
8
10

Fig. 8

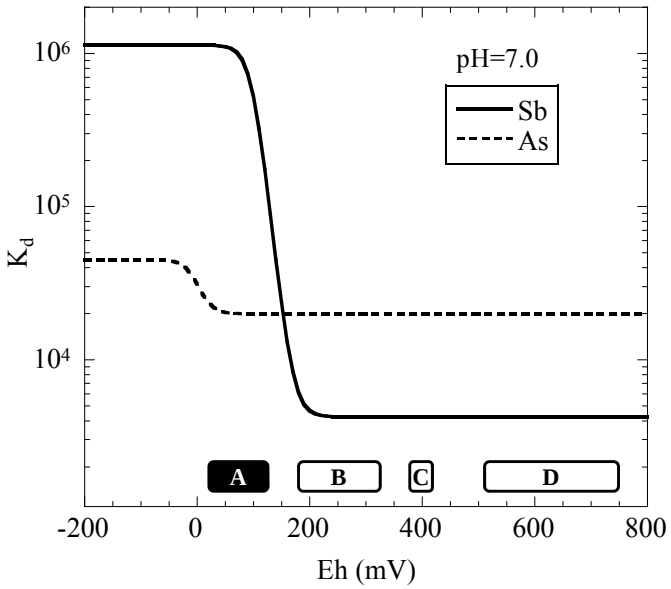

A: Mitsunobu et al., (2006); B: Masson et al, (2009); C: This study, Ichonokawa-Kamo river systems; D: Manaka et al., (2007)

Fig. 9

Tables.

Table 1 Concentration of major ions in Kamo and Ichinokawa river (mg L^{-1})

Sampling station	Cl^-	NO_3^-	SO_4^{2-}	Na^+	Ca^{2+}	Mg^{2+}
I-1	2.7	4.0	10.7	4.3	11.9	3.3
I-2	3.3	4.3	17.9	5.2	14.8	4.5
I-3	3.7	4.2	17.8	6.8	15.3	4.7
K-1	2.8	3.2	7.6	4.1	11.8	1.5
K-2	3.3	3.3	8.5	4.8	12.7	1.8
K-3	2.9	3.2	8.5	4.8	13.0	1.8
K-4	3.1	3.0	9.2	5.0	14.1	1.9
K-5	3.5	3.2	9.1	6.0	13.7	2.0

Table 2 Mass balance of antimony, arsenic and major elements

Stations	Sb	As	Na	Mg	Ca	Cl	SO_4
K2 (kg d^{-1})	0.11	0.20	3500	1300	9100	2400	6100
I3 (kg d^{-1})	4.0	0.11	240	170	540	130	170
K4 (kg d^{-1})	2.9	0.25	3800	1400	11000	2400	6900
Excess or Deficiency (%)	-29	-20	1.6	-4.8	14	-5.1	10

Table 3Concentrations of antimony and arsenic in dissolved and particulate fractions in river water and particulate matter. Distribution coefficients (Kd) calculated from dissolved fractions and particulate matter values were also given.

Stations	Sb				As			
	Dissolved ($\mu g\ L^{-1}$)	Particulate ($\mu g\ L^{-1}$)	Particulate matter ($\mu g\ kg^{-1}$)	Kd ($L\ kg^{-1}$)	Dissolved ($\mu g\ L^{-1}$)	Particulate ($\mu g\ L^{-1}$)	Particulate matter ($\mu g\ kg^{-1}$)	Kd ($L\ kg^{-1}$)
K2	0.16	0.00007	160	1.0×10^3	0.28	0.002	4790	1.7×10^4
I3	113	0.004	3880	34	3.21	0.003	3020	9.4×10^2
K4	3.9	0.0006	589	1.5×10^2	0.33	0.009	8570	2.6×10^4

Table 4 EXAFS parameters for Sb in sediment at St. I-2

Shell	CN	R (Å)	ΔE_0 (eV)	σ^2 (x 10^3 Å^2)	Residual (%)
Sb-O	5.6 ± 1.3	1.986 ± 0.017		5.0 ± 0.7	
Sb-Fe1	1.5 ± 0.1	3.115 ± 0.041	6.6 ± 2.4	4.9*	0.7
Sb-Fe2	1.4 ± 0.1	3.609 ± 0.041		4.9*	

*Fixed.; CN: coordination number

Table 5 Antimony and arsenic distribution in each phase

	Sb (mg kg^{-1})	As (mg kg^{-1})	Phase
Fraction 1	6.94	2.51	Carbonate and exchangeable
Fraction 2	153	53.1	Poorly cystalline Fe-oxyhydroxide
Fraction 3	64.6	15.7	Crystalline Fe-oxyhydroxide
Fraction 4	140	0.338	Al-oxide and clay minerals
Fraction 5	167	16.6	Primary and secondary minerals

Supplementary data

Comparison of antimony and arsenic behavior in an Ichinokawa river water-sediment system

Satoshi Asaoka,[1,*,†] Yoshio Takahashi,[1] Yusuke Araki,[1] and Masaharu Tanimizu[2]

1) Department of Earth and Planetary Systems Science, Graduate School of Science, Hiroshima University, 1-3-1 Kagamiyama, Higashi-Hiroshima, Japan 739-8526

2) Kochi Institute for Core Sample Research, Japan Agency for Marine-Earth Science and Technology

200 Monobe Otsu, Nankoku, Japan 783-8502

[†]Present address: Research Center for Inland Seas, Kobe University

5-1-1 Fukaeminami, Higashinada, Kobe, Japan 658-0022

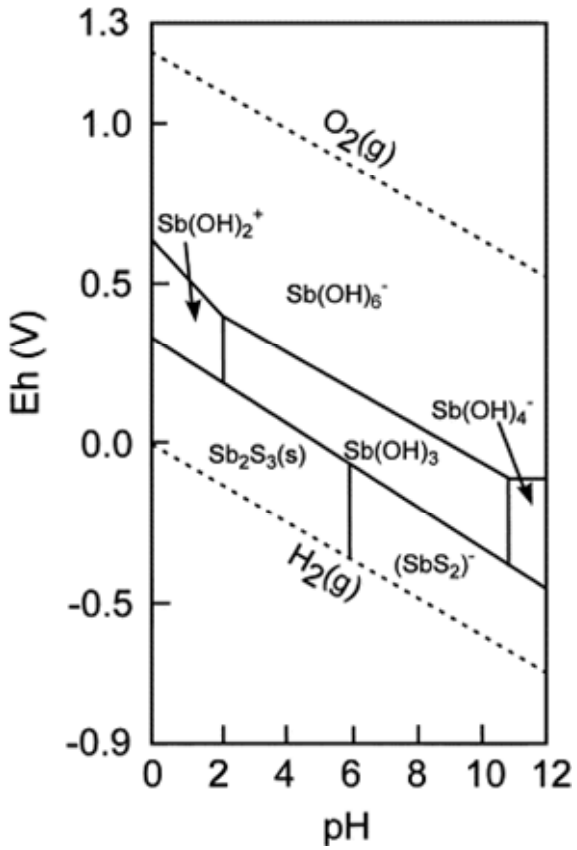

Figure S1 Eh-pH diagram of antimony in the Sb–S–H_2O system (Filella et al., 2002a).

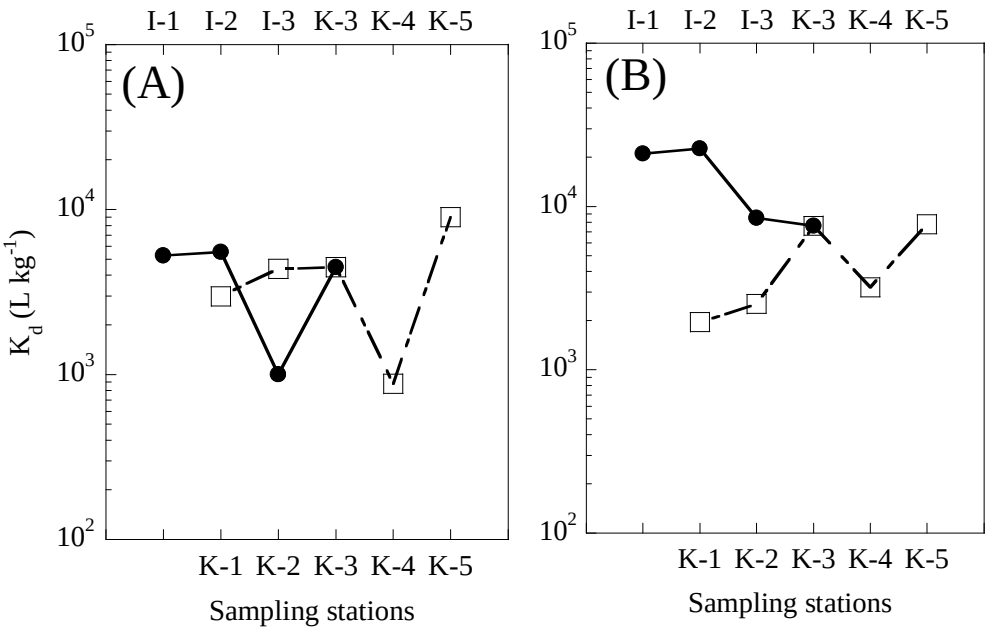

Figure S2 Distribution coefficients antimony (A) and arsenic (B) between aqueous phase and the sediments along Kamo and Ichinokawa river system.

□ : Kamo river; ●:Ichinokawa river

Table S1 Antimony species ratio in Kamo and Ichinokawa river sediments

Sampling Stations	Sb(III) %	Sb(V) %
I-1	27	73
I-2	16	84
I-3	40	60
K-3	34	66
K-5	21	79

Table S2 Arsenic species ratio in Kamo and Ichinokawa river sediments

Sampling Stations	As(III) %	As(V) %
I-1	16	84
I-2	20	80
I-3	29	71

Table S3 Iron species ratio in Kamo and Ichinokawa river sediments

Sampling Stations	Biotite (%)	Ferrihydrite (%)
I-1	44	56
I-2	38	62
I-3	33	67
K-1	54	48
K-2	53	47
K-3	58	42
K-4	52	48
K-5	57	44